

# The Influence of Heat Treatment and Chemical Composition on the Structure and Mechanical Properties of Thick-walled Ductile Iron Castings

**M. Trepczyńska-Lent**

Department of Materials Science and Engineering, Mechanical Engineering Faculty,  
UTP University of Science and Technology, Al. prof. S. Kaliskiego 7, 85-796 Bydgoszcz, Poland  
Corresponding authors. E-mail address: malgorzata.trepczynska-lent@utp.edu.pl

Received 28.05.2018; accepted in revised form 17.10.2018

## Abstract

In this work, the effects of 75 mm thick cast iron, (casting mould YIV) composition (Cu) and heat treatment were investigated on the microstructure and mechanical properties (hardness, elongation, tensile strength, yield strength) of ductile iron castings. As a result of adding Cu, the amount of pearlite is at 80% reduces of amount of ferrite. Normalizing of non-alloy cast iron increases the amount of pearlite to 70%. It also, increases tensile strength (659 MPa) and hardness (248 HB). Studied metallographic crosssections were made from the grip sections of the tensile specimens. The structure composition and the characteristics of graphite were determined by computer image analysis. Measurements of graphite of non-alloy cast iron after normalizing and in cooper cast iron indicate the approximate amount of precipitates of graphite and their approximate average diameters. The applied normalizing and the additive alloy (Cu) were established to give comparable mechanical properties and structure of matrix in thick-walled castings.

**Keywords:** Thick-walled castings, Cast iron, Structure, Mechanical properties

## 1. Introduction

Increase of interest in thin and thick wall ductile iron casting solidification can be observed in recent years.

Thick wall ductile iron castings are, for example, the bodies of: impellers and high-pressure pumps, housings of propellers for a wind power plant.

In usual commercial applications ductile cast iron in cast condition microstructure consists spheroidal graphite, ferrite and perlite matrix. Such microstructure is significantly important on mechanical properties [1, 2].

The properties of as-cast ductile iron are controlled mainly by cooling rate, along with chemical composition and melt treatment [1, 3].

Growth of graphite nucleates is controlled by austenite dendrites [1, 4].

Austenite, which is formed during solidification go through the solid-state transformation at eutectoid temperature, which is modifying the solidified structure and then lead to other complexities in solidification morphology [5].

In the stable eutectoid reaction, austenite is decomposed into graphite and ferrite. The ferrite is nucleating and grows symmetrically around the spheroidal graphite at the graphite/austenite interface, during the ferritic reaction [6].

Diffusion of carbon through the ferrite shell controls this growth. Consequently, this is rather slow process and the temperature of the metastable eutectoid could be reached before the complete transformation of austenite [6].

The proportion of ferrite to pearlite in the matrix and the morphology of graphite have impact on the mechanical properties of ductile iron castings [7]. The cooling rate throughout eutectoid transformation, alloying elements and nodule count have an impact on that [1, 8]. The softer ferrite gives higher ductility but lowers tensile strength in comparison to pearlite [9]. The time span between spheroidal treatment and pouring has a major effect on elongation. It effects less the hardness of castings and tensile strength [10].

The alloying elements such as Cu, Mn, Sn, Sb and Cr increase tensile strength and hardness and decrease ductility and impact energy. It is caused by an increase in the amount of pearlite along with decrease in ferrite. Even small changes in the amount of those elements show significant change in mechanical properties of ductile iron. Copper is a strong pearlite promoter; its addition up to 1% converts ferritic structure into pearlitic structure. Silicon is a strong solid solution strengthener; reducing undercooling and avoiding carbide formation by nucleating graphite. It increases volume fraction of ferrite and nodule count. Manganese increases strength and hardness by stabilizing pearlite. Although it promotes carbides in heavy sections. It segregates at grain boundaries and consequently increases hardenability [11-16].

Several mechanical properties, especially elongation, are reduced with the increase of wall-thickness and weight of the cast iron castings. That degradation of graphite morphology in the thermal centre of heavily wall-thick ductile cast iron castings is usually caused magnesium chemistry segregation and fading. The difference between the test coupons separately cast and the samples cut from the heavy castings, in mechanical properties, is caused by this fact. It also results in problems with obtaining a reliability of ductile cast iron castings. Also, the graphite morphology is essential; deviation from spheroidal shape reduces the impact properties and ductility [9]. This degradation is presumed to be related to the microstructural changes through the wall-thickness, but this subject need further systematic research in heavy castings [17, 18].

Disintegrated graphite might be present in very slowly cooled cross-sections of the casts. The chunky graphite – degraded form of the graphite – may form in the casts made of ductile iron with large thermal point. This happens due to the different solidification rate. The presence of spheroidal form of the graphite in the structure of the ductile iron assumes the excellent mechanical properties of this iron – mainly the tensile strength and ductility. For the chunky graphite these properties are significantly lower. Its presence is not allowed in the structure of the ductile iron. Chunky graphite is formed inside the cells. The cell boundaries might also contain the well-formed spheres. This is a case of the thicker walls of the cast [19-21]. Chunky graphite might be removed, and the structure obtained might be containing fully spheroidal graphite. This can be obtained by adding the elements that support the development of the inter-cell lamellar graphite.

Because of the supporting the inter-cell lamellar graphite formation these elements can be classified in two groups. The elements that support the chunky graphite formation: Ca, Ce, Ni,

Si. The other group contains the elements that support the formation of the lamellar inter cell graphite formation: Al, As, Bi, Cd, Cu, Pb, Sb, Sn [22, 23].

The current paper presents the results of normalizing non-alloyed cast iron and adding the Cu element to thick wall ductile cast iron castings.

## 2. Experimental procedure

Mechanical properties ( $R_m$ ,  $R_{p0.2}$ ,  $A_5$ ) and the hardness distribution were determined and the microstructure on cross sections of standard YIV castings with a wall thickness of 75 mm was evaluated.

### 2.1. Research material

For the study, two types of ductile cast iron were used. In Table 1 the chemical composition of the cast iron is shown. In the Foundry "Śrem" S.A. fusible ingots of EN-GJS-400-15 (non-alloyed) ferritic iron and perlitic-ferritic EN-GJS-600-03 (alloyed) were made. They were cast into YIV sample molds (wall thickness 75 mm). The size of the test sample is shown in Figure 1 (according to PN-EN 1563: 2012). The method of cutting the samples for testing is shown in Figure 2.

Two plates were cut to measure the hardness. Measurements of mechanical properties ( $R_m$ ,  $R_{p0.2}$ ,  $A_5$ ) were carried out on six strength samples made as shown in Figure 2.

The microstructure of casting non-alloyed cast iron is shown in Figure 3.

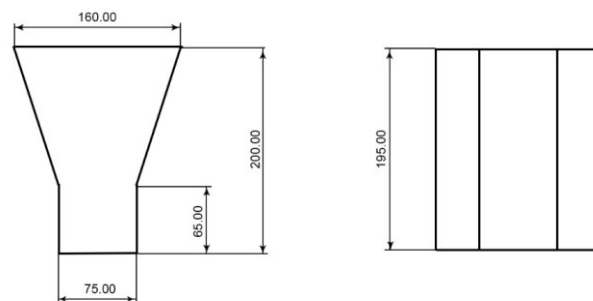


Fig. 1. Dimensions of the test ingot YIV

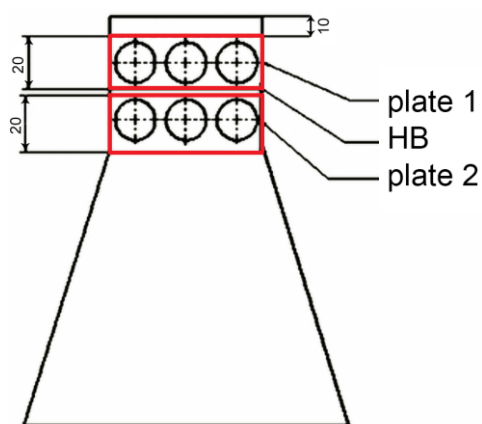


Fig. 2. Plates (red) cutting method

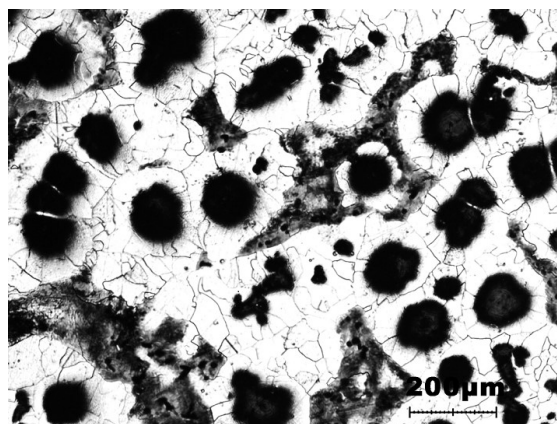


Fig. 3. Microstructure of non-alloyed cast iron, Nital etched

Table 1.

Chemical composition [wt. %]

| cast iron   | C    | Si   | Mn   | P     | S     | Cr   | Cu   | Ti   | Mg    | Ni    | Mo    | V     | Al     | $K_G''$ | $S_c$ | $C_E$ |
|-------------|------|------|------|-------|-------|------|------|------|-------|-------|-------|-------|--------|---------|-------|-------|
| non-alloyed | 3.82 | 3.21 | 0.17 | 0.059 | 0.019 | 0.01 | 0.12 | 0.19 | 0.047 | 0.008 | 0.002 | 0.009 | 0.0026 | 12.0    | 1.18  | 2.82  |
| alloyed     | 3.39 | 2.62 | 0.29 | 0.042 | 0.010 | -    | 0.51 | -    | 0.046 | 0.072 | -     | -     | -      | 10.9    | 0.99  | 2.49  |

 $K_G''$  – graphitization carbon equivalent by Girshovich [24] $S_c$  – degree of eutectic saturation $C_E$  – eutectic carbon equivalent

## 2.2. Heat treatment

Normalizing of non-alloyed cast iron was made in a PSK7 furnace, which accuracy was  $\pm 5^\circ\text{C}$ . The normalizing scheme is shown in Figure 4.

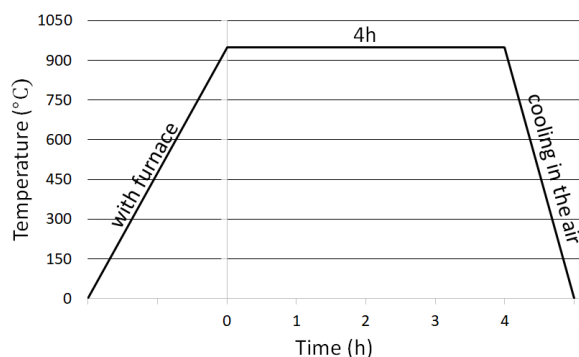


Fig. 4. Diagram of the normalizing

## 3. Experimental results

Hardness measurements were made on cut-out plates 1 and 2 (Fig. 2). Tensile tests were performed on fivefold strength sample with a diameter of 10 mm using the INSTRON 8502. The test was carried out and the values of  $A_5$ ,  $R_m$  and  $R_{0.2}$  were read from the graphs shown in Table 2.

Table 2.

Results of the tensile test of researched cast iron after casting and normalizing

| Cast iron   | State              | $A_5$ % | $R_m$ MPa | $R_{0.2}$ MPa | HB   |
|-------------|--------------------|---------|-----------|---------------|------|
| non-alloyed | Casting            | 11.00   | 467       | 357           | 171  |
|             | min                | 9.40    | 458       | 355           | 145  |
|             | max                | 10.54   | 478       | 359           | 180  |
|             | standard deviation | 2.05    | 8.94      | 1.43          | 0.65 |
|             | Normal.            | 2.52    | 654       | 503           | 248  |
|             | min                | 2.35    | 603       | 497           | 246  |
| alloyed     | max                | 2.80    | 685       | 515           | 249  |
|             | standard deviation | 0.64    | 31.30     | 6.80          | 0.12 |
|             | Casting            | 2.98    | 590       | 450           | 244  |
|             | min                | 1.89    | 542       | 437           | 239  |
|             | max                | 4.10    | 637       | 456           | 246  |
|             | standard deviation | 0.84    | 37.37     | 7.51          | 0.23 |

The Figures 6÷9 show the microstructure of non-alloyed cast iron after normalizing at the center and the edge of plate. The Figures 10÷13 show the microstructure of copper cast iron at the center and the edge of plate.

Using the image analysis NIS-Elements graphite measurements were made. Results are shown in Table 3. They are averaged measurements taken in five different areas of the test plate 1 from the center to its edges.

Measurements 1÷5 are referring to graphite parameters for non-alloyed cast iron after casting; measurements 6÷10 – non-alloy cast iron after normalizing; measurements 11÷15 – alloyed cast iron.

Column E shows the value of the quotient of the surface area under study to the average graphite diameter (column value B / column C value). Column F shows the degree of approximation of the graphite shape to the spherical shape.

## 4. Discussion

Non-alloyed cast iron has ferritic-perlite structure with a content of about 15 % perlite. The hardness of this cast iron is ranged from 157.1 to 177.3 HB after casting. After normalizing, significant increase in the amount of perlite content by about 70 %, was observed. Therefore, there was a general increase in hardness, of about 80 HB and it ranged from 246.7 up to 247.5 HB.

Table 3

Parameters of graphite measurements

| A                     | B                               | C                          | D            | E            | F                               | G |
|-----------------------|---------------------------------|----------------------------|--------------|--------------|---------------------------------|---|
| Area, $\mu\text{m}^2$ | Average diameter, $\mu\text{m}$ | Fill area, $\mu\text{m}^2$ | Quotient B/C | Roundness    | Amount of graphite precipitates |   |
| 1                     | 151.43                          | 174580.2                   | 12.31        | 0.827        | 26                              |   |
| 2                     | 153.23                          | 171750.9                   | 12.51        | 0.833        | 21                              |   |
| 3                     | 152.76                          | 171640.6                   | 12.52        | 0.832        | 19                              |   |
| 4                     | 151.78                          | 171643.6                   | 12.52        | 0.836        | 19                              |   |
| 5                     | 150.78                          | 171652.1                   | 12.52        | 0.829        | 21                              |   |
| <b>Av.</b>            | <b>152.00</b>                   | <b>172253.4</b>            | <b>12.48</b> | <b>0.831</b> | <b>21</b>                       |   |
| 6                     | 152.45                          | 171653.8                   | 12.52        | 0.862        | 23                              |   |
| 7                     | 148.72                          | 174623.1                   | 12.31        | 0.817        | 29                              |   |
| 8                     | 145.48                          | 174588.2                   | 12.31        | 0.792        | 31                              |   |
| 9                     | 142.76                          | 174527.3                   | 12.31        | 0.803        | 33                              |   |
| 10                    | 139.88                          | 174436.2                   | 12.32        | 0.841        | 39                              |   |
| <b>Av.</b>            | <b>145.86</b>                   | <b>173965.7</b>            | <b>12.35</b> | <b>0.823</b> | <b>31</b>                       |   |
| 11                    | 137.92                          | 174357.1                   | 12.33        | 0.863        | 41                              |   |
| 12                    | 136.54                          | 173892.1                   | 12.36        | 0.875        | 43                              |   |
| 13                    | 131.17                          | 176632.1                   | 12.17        | 0.797        | 35                              |   |
| 14                    | 129.58                          | 175472.3                   | 12.25        | 0.844        | 48                              |   |
| 15                    | 129.12                          | 175743.1                   | 12.23        | 0.795        | 30                              |   |
| <b>Av.</b>            | <b>132.87</b>                   | <b>175219.3</b>            | <b>12.27</b> | <b>0.835</b> | <b>39</b>                       |   |

Alloyed cast iron has pearlite-ferrite structure with the amount of about 20 % of ferrite. The average hardness of cooper cast iron – 244 HB – is very close to the values of non-alloyed cast iron

after normalizing. Cast iron after the casting has the structure resulting from primary and secondary crystallization (solid state). The thick-walled castings are characterised by strong chemical microsegregation and structural segregation. This have disadvantageous effect on all properties of castings. Segregation in thick-walled castings and changes in graphite shape determine the structure, and therefore the properties of the cast. Microsegregation can be reduced by heat treatment. The heat treatment used in this work include an austenitizing treatment. During this process homogenizing of the cast iron matrix metal occurs and especially the equalization of silicon and manganese concentration.

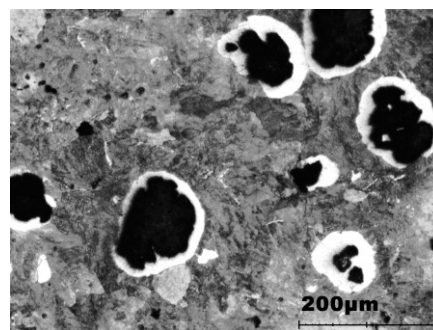


Fig. 6. Microstructure of normalized non-alloyed cast iron, center of plate 1, Nital etched

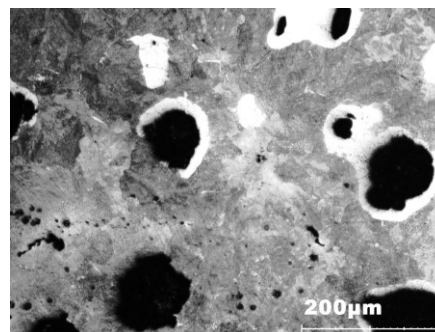


Fig. 7. Microstructure of normalized non-alloyed cast iron, edge of plate 1, Nital etched

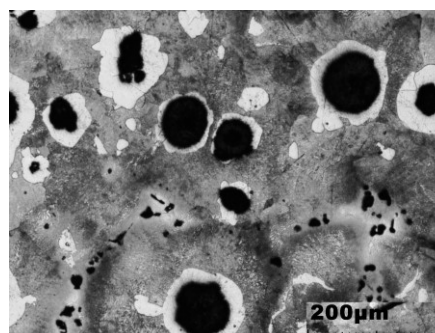


Fig. 8. Microstructure of normalized non-alloyed cast iron, center of plate 2, Nital etched



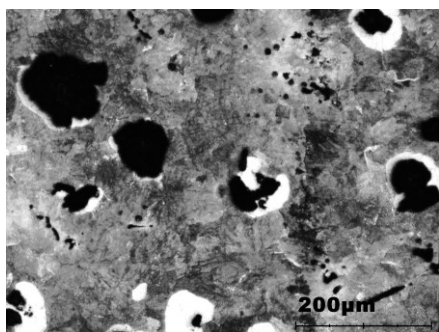


Fig. 9. Microstructure of normalized non-alloyed cast iron, edge of plate 2, Nital etched

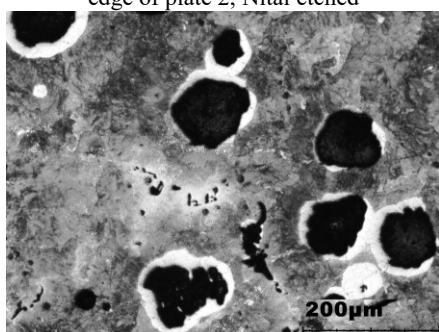


Fig.10. Microstructure of alloyed cast iron, center of the plate 1, Nital etched

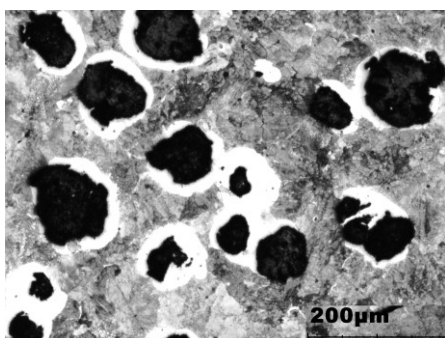


Fig. 11. Microstructure of alloyed cast iron, edge of the plate 1, Nital etched

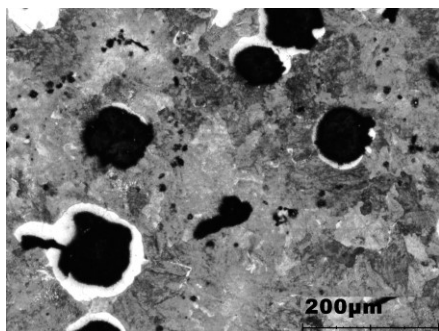


Fig. 12. Microstructure of alloyed cast iron, center of the plate 2, Nital etched

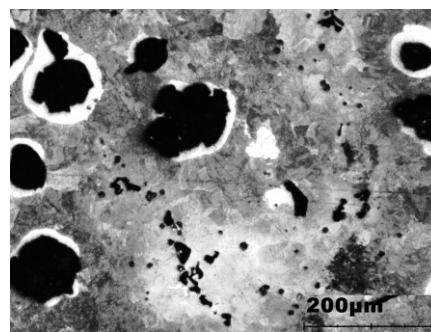


Fig. 13 Microstructure of alloyed cast iron, edge of the plate 2, Nital etched

Alloyed cast iron after casting, has a much greater homogeneity in hardness distribution than non-alloy cast iron. In general, perlitzation of the matrix is induced by the copper addition.

Non-alloyed cast iron after normalizing and alloyed cast iron have a similar range of values of  $R_m$  (Tab.2). In the center of the plate the highest value of this parameter is observed. For this parameter the highest standard deviation has been over 30. The most homogeneous results were obtained for the parameter  $A_5$

The addition of copper inhibited the growth of graphite (Tab. 3). Measurements of graphite of non-alloyed cast iron after normalizing (Tab. 3, line 6÷10) and in alloyed cast iron (Tab. 3, line 11÷15) they indicate the approximate amount of precipitates of graphite (31 and 39, respectively) and their approximate average diameters (146  $\mu\text{m}$  and 133  $\mu\text{m}$ , respectively).

## 5. Conclusions

The properties of ductile iron are mainly determined by their microstructure, chemical composition of the melt and section thickness of the casting. The microstructure and consequently mechanical properties (particularly hardness and tensile strength) might be improved in thick wall ductile iron castings by increasing the amount of copper. The addition of Cu increases the amount of pearlite up to 80% in the ductile iron castings.

Hardness can be significantly changed by heat treatment with high temperature treatment. During long-lasting austenitization there is a reduction in micro-segregation and structural segregation.

An effective way to change the properties in thick-walled castings is the addition of copper.

The place of taking samples in the thick-walled casting has an influence on the values of the mechanical properties  $R_m$ ,  $R_{p0.2}$ ,  $A_5$ . During crystallization, with the growth of the cooling rate, the values of these properties improve.

## References

- [1] Campbell, J.(2015). *Complete Casting Handbook*. 2<sup>nd</sup> Edition. Butterworth-Heinemann.

- [2] Swain, S.K. & Sen, S. (2011). Study of microstructure of thick wall ductile iron castings. *Journal of Metallurgy and Materials Science*. 53(2), 133-137.
- [3] Bockus, S. & Zaldarys, G. (2011). Evaluation of Producing Technique Factors Affecting the Matrix Microstructure of As-Cast Ductile Iron Castings. *Metallurgija*. 50(1), 9-12.
- [4] Campbell, J.(2009) A Hypothesis for cast iron microstructures, *Metallurgical and Materials Transactions B*. 40B, 786-801.
- [5] Mrvar, P., Petric, M. & Medved, J. (2011). Influence of cooling rate and alloying elements on kinetics of eutectoid transformation in spheroidal graphite cast iron. *Key Engineering Materials*. 457, 163-168.
- [6] Lacaze, J., Castro, M. & Esoult, G.L. (1998). Solidification of spheroidal graphite cast iron-II numerical simulation. *Acta Materialia*. 6, 997-1010.
- [7] Serrallach, J., Lacaze, J., Sertucha, J. Suarez, R. & Monzon, A. (2011). Effect of selected alloying elements on mechanical properties of pearlitic nodular cast irons, Science and Processing of Cast Iron IX. *Key Engineering Materials*. 457, 361-366.  
DOI: 10.4028/www.scientific.net/KEM.457.361.
- [8] Goodrich, G.M. & Lobenhoger, R.W. (2007). Effect of cooling rate on pearlitic ductile iron mechanical properties. *AFS Transactions*. 115(05), 07-045.
- [9] Bockus, S. & Dobrovolskis, A. (2004). Peculiarity of producing ferritic ductile iron castings. *Materials Science*. (Medziagotyra). 10(1), 3-6.
- [10] Soiniński, M.S. & Derda, A. (2008). The influence of selected elements on mechanical properties of ferritic ductile iron. *Archives of Foundry Engineering*. 8(3), 149-152.
- [11] Silman, G.I., Kamynin, V.V. & Goncharov, V.V. (2007). On the mechanisms of copper effect on structure formation in cast iron. *Metal Science and Heat Treatment*. 49(7-8), 387-393. <https://doi.org/10.1007/s11041-007-0072-z>.
- [12] Gonzaga, R.A. & Carrasquilla, J.F. (2005). Influence of an appropriate balance of the alloying elements on iron. *Journal of Materials Processing Technology*. 162-163, 293-297.
- [13] Stawarz, M. (2017). SiMo Ductile Iron Crystallization Process. *Archives of Foundry Engineering*. 17(1), 147-152.  
DOI:10.1515/afe-2017-0027.
- [14] Pirowski, Z., Wodnicki, J., Olszyński, J., Gościński, M. & Dudziak, B. (2012). Effect of boron additive on hardenability changes of ductile iron with isothermal transformation for the thick-walled castings. *Journal of Research and Applications in Agricultural Engineering*. 57(2), 153-155.
- [15] Chinakhov, D.A. (2014). Structure and mechanical properties of Cu-alloyed cast iron. *Applied Mechanics and Materials*. 682, 178-182.
- [16] Stawarz, M. (2013). Influence of technological parameters on the microstructure of the silicon cast iron, In Metal 2013: 22nd International Conference on Metallurgy and Materials, Ostrava. TANGER 2013, pp. 92-96 .
- [17] Xue-Zheng, W., Xiaro-Rui, S., Ying, Z. (2012). Study on productive technology of greensand mold and thick-walled small piece for nodular cast iron. *Advanced Materials Research*. 490-495, 3545-3548. <https://doi.org/10.4028/www.scientific.net/AMR.490-495.3545>.
- [18] Fraš, E., Górný, M. & Lopez, H.F. (2007). Graphite nodule and cell count in cast iron. *Archives of Foundry Engineering*. 7(3), 47-52.
- [19] Zhe, L., Weiping, Ch. & Yu, D. (2012). Influence of cooling rate and antimony addition content on graphite morphology and mechanical properties of a ductile iron. *China Foundry*. 9(2), 114-118.
- [20] Falat, L., Čiripová, L., Kepič, J., Buršik, J. & Podstranská, I. (2014). Correlation between microstructure and creep performance of artensitic/austenitic transition weldment in dependence of its post-weld heat treatment. *Engineering Failure Analysis*. 40, 141-152.
- [21] Falat, L., Kepič, J., Čiripová, L., Ševc, P., & Dlouhý, I. (2016). The effects of postweld heat treatment and isothermal aging on T92 steel heat-affected zone mechanical properties of T92/TP316H dissimilar weldments. *Journal of Materials Research*. 31, 1532-1543.
- [22] Karsay, S.I. (1992). Gusseisen mit Kugelgraphit I., QIT-FERET TITANE INC.
- [23] Nakae, H., Jung, S. & Shin, H.C. (2008). Formation mechanism of chunky graphite and its preventive measure. *Journal of Materials Science & Technology*. 24, 289-295.
- [24] Girshovich, N.G. (1966). Crystallisation and properties of cast iron in castings. (Kristalizacija i svojstva czuguna w otliwkach). *Maszynostrojenie, Moskwa – Leningrad*, 562.